

Supporting Information

Pressure-induced remarkable luminescence switch of a dimer form of donor–acceptor–donor triphenylamine (TPA) derivative

Aisen Li,^{a,b,#} Ning Chu,^{a,#} Jianwei Liu,^c Hao Liu,^d Jing Wang,^a Shuping Xu,^a Haining Cui,^b Hongyu Zhang,^d Weiqing Xu,^{a*} and Zhiyong Ma^{c*}

a. State Key Laboratory of Supramolecular Structure and Materials, Institute of Theoretical Chemistry, Jilin University, Changchun 130012, P. R. China

b. College of Physics, Jilin University, Changchun 130012, P. R. China

c. Beijing State Key Laboratory of Organic-Inorganic Composites, College of Chemical Engineering, Beijing University of Chemical Technology, Beijing 100029, P. R. China.

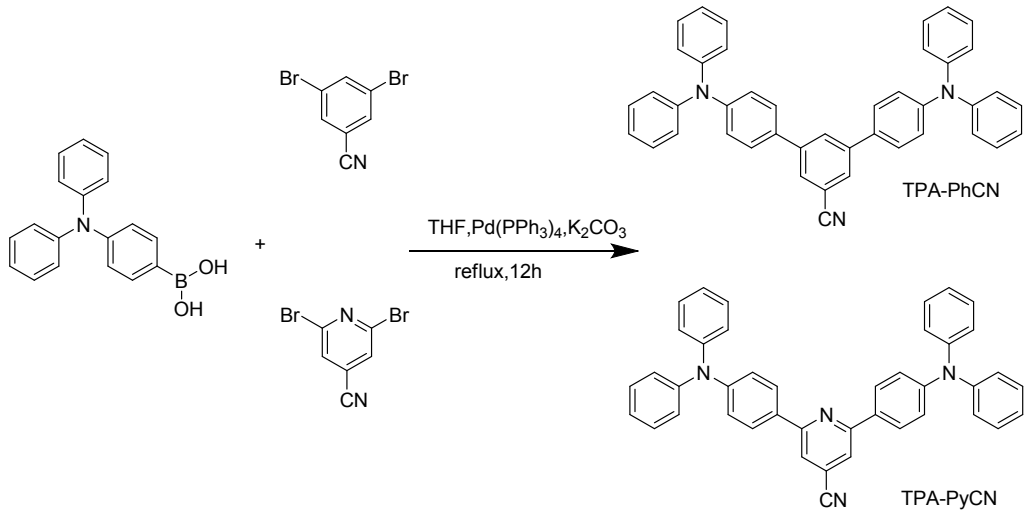
d. State Key Laboratory of Supramolecular Structure and Materials, College of Chemistry, Jilin University, Changchun, P. R. China 130012

#. These authors contributed equally to this work.

Content

1. Synthesis of TPA-Ph-CN and TPA-Py-CN	3
2. Characterization results	4
3. Single crystal parameters.....	8
4. Raman spectra of TPA-Ph-CN and TPA-Py-CN	9
5. Absorption spectra of TPA-Ph-CN and TPA-Py-CN	12
6. HOMOs and LUMOs of TPA-Ph-CN and TPA-Py-CN.....	13
7. Fluorescent spectra of TPA-Ph-CN and TPA-Py-CN.....	14
8. Structural analysis of TPA-Ph-CN and TPA-Py-CN.....	15
9. Time-resolved photoluminescence (TRPL) of TPA-Py-CN	16
10. Fluorescent spectra of TPA-Ph-CN and TPA-Py-CN under hydrostatic pressure.....	17
11. Raman spectra of TPA-Py-CN under hydrostatic pressure.....	19
12. Theoretical calculations of TPA-Py-CN under pressure.....	21
References	24

1. Synthesis of TPA-Ph-CN and TPA-Py-CN.



Scheme S1. The synthetic route for TPA-Ph-CN or TPA-Py-CN.

TPA-Ph-CN

4-(diphenylamino)phenylboronic acid (0.578 g, 2.0 mmol), 3,5-dibromobenzonitrile (0.261 g, 1.0 mmol), tetrakis(triphenylphosphine)palladium(0) (0.099 g, 0.09 mmol) and potassium carbonate (0.470 g, 3.46 mmol) were added in a Schlenk tube. After thorough deoxygenation, 20.0 mL of distilled THF and 3.0 mL of deionized water were added into the sealed tube by injection. The solution was kept stirring at 60°C for 24 h. After cooling to room temperature, the product was separated through extraction. Then, after evaporation of the solvent, the crude product was purified by column chromatography (DCM: petroleum ether=1:3, v/v) to afford TPA-Ph-CN (white powder, yield 31%).

TPA-Py-CN

4-(diphenylamino)phenylboronic acid (0.252 g, 0.87 mmol), 2,6-dibromopyridine-4-carbonitrile (0.114 g, 0.44 mmol), tetrakis(triphenylphosphine)palladium(0) (0.030 g, 2.62 nmol) and potassium carbonate (0.362 g, 2.62 mmol) were added in a Schlenk

tube. After thorough deoxygenation, 20.0 mL of distilled THF and 3.0 mL of deionized water were added into the sealed tube by injection. The solution was kept stirring at 60 °C for 24 h. After cooling to room temperature, the product was separated through extraction. Then, after evaporation of the solvent, the crude product was separated through extraction and then purified by column chromatography (DCM: petroleum ether=1:5, v/v) to afford TPA-Py-CN (yellow powder, yield= 47%).

2. Characterization results.

TPA-Ph-CN

¹H NMR: (500 MHz, CDCl₃) δ/ppm: 7.96 (s, 1H), 7.77 (d, J = 1.6 Hz, 2H), 7.49 (d, J = 8.6 Hz, 4H), 7.35 – 7.29 (m, 8H), 7.20 – 7.14 (m, 12H), 7.10 (q, J = 7.7 Hz, 4H).

¹³C NMR: (126 MHz, CDCl₃) δ/ppm: 148.33 (s), 147.38 (s), 142.43 (s), 132.34 (s), 129.29 (d, J = 32.4 Hz), 128.00 (d, J = 44.3 Hz), 124.82 (s), 123.40 (d, J = 11.5 Hz), 119.10 (s), 113.32 (s).

MS Calcd. For C₄₃H₃₁N₃ [M+H]⁺: 590.71. Found: 590.090.

TPA-Py-CN

¹H NMR: (500 MHz, CDCl₃) δ/ppm: 7.97 (d, J = 8.8 Hz, 4H), 7.70 (s, 2H), 7.30 (t, J = 7.9 Hz, 8H), 7.15 (dd, J = 8.2, 4.2 Hz, 12H), 7.08 (t, J = 7.3 Hz, 4H).

¹³C NMR: (126 MHz, CDCl₃) δ/ppm: 157.55 (s), 149.78 (s), 147.15 (s), 130.66 (s), 129.45 (s), 127.92 (s), 125.17 (s), 123.76 (s), 122.38 (s), 118.19 (s).

MS Calcd. For C₄₂H₃₀N₄ [M+H]⁺: 591.70. Found: 591.030.

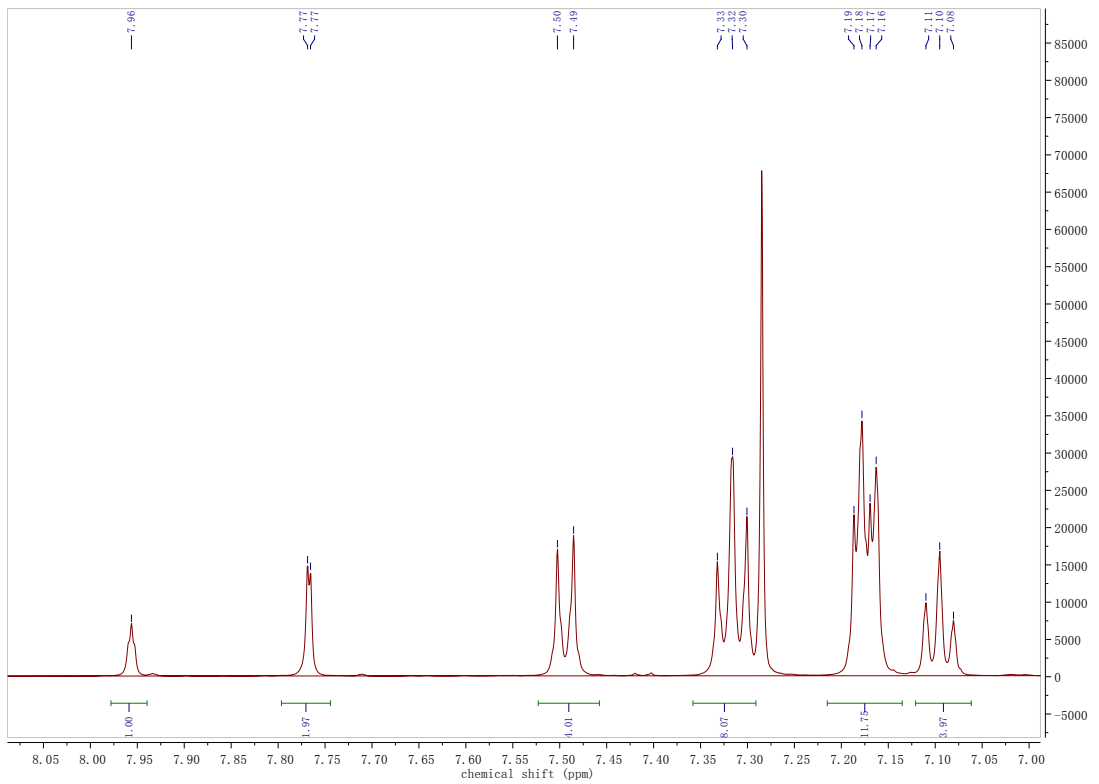


Figure S1. ^1H NMR spectrum of TPA-Ph-CN.

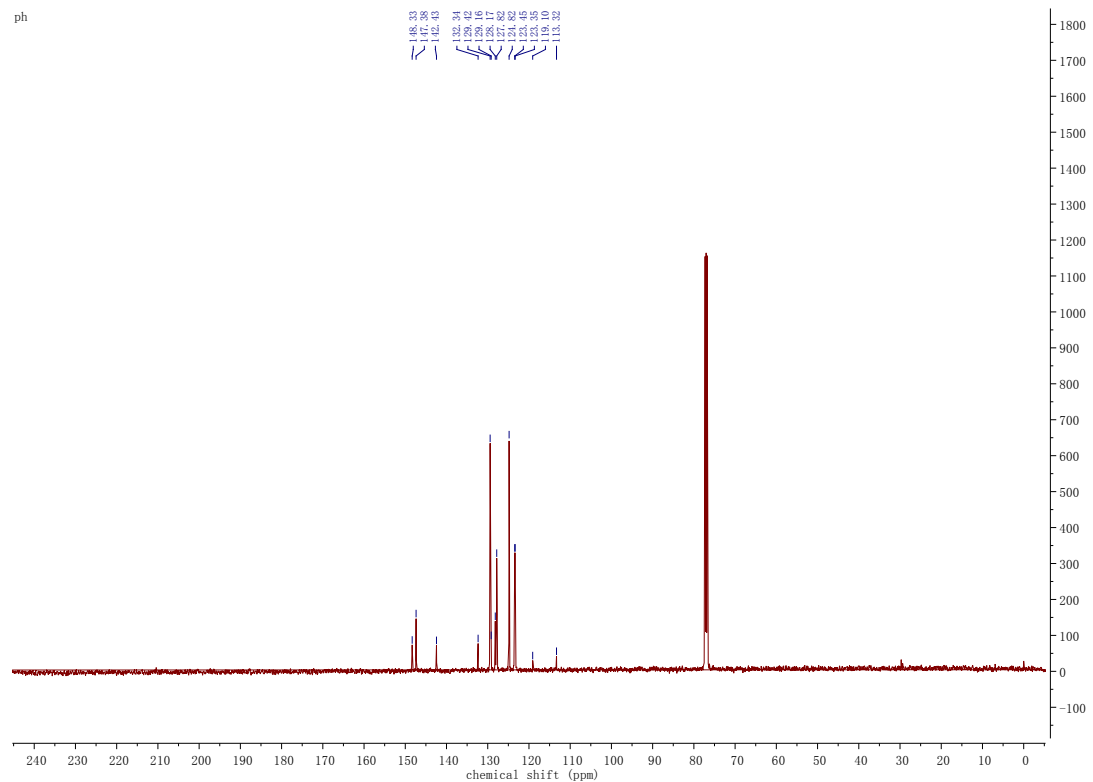


Figure S2. ^{13}C NMR spectrum of TPA-Ph-CN.

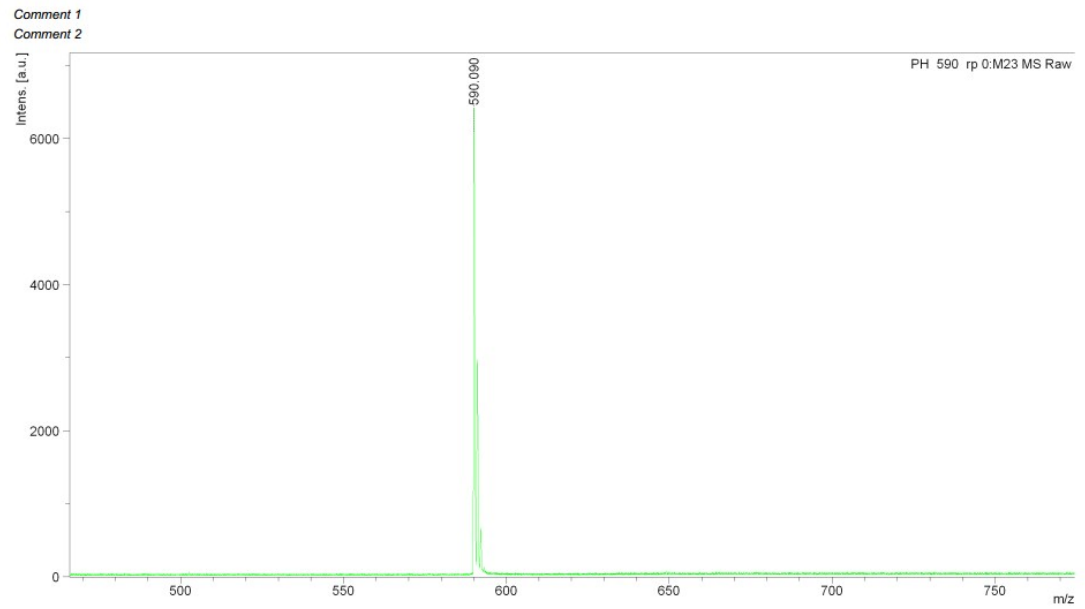


Figure S3. MS spectrum of TPA-Ph-CN.

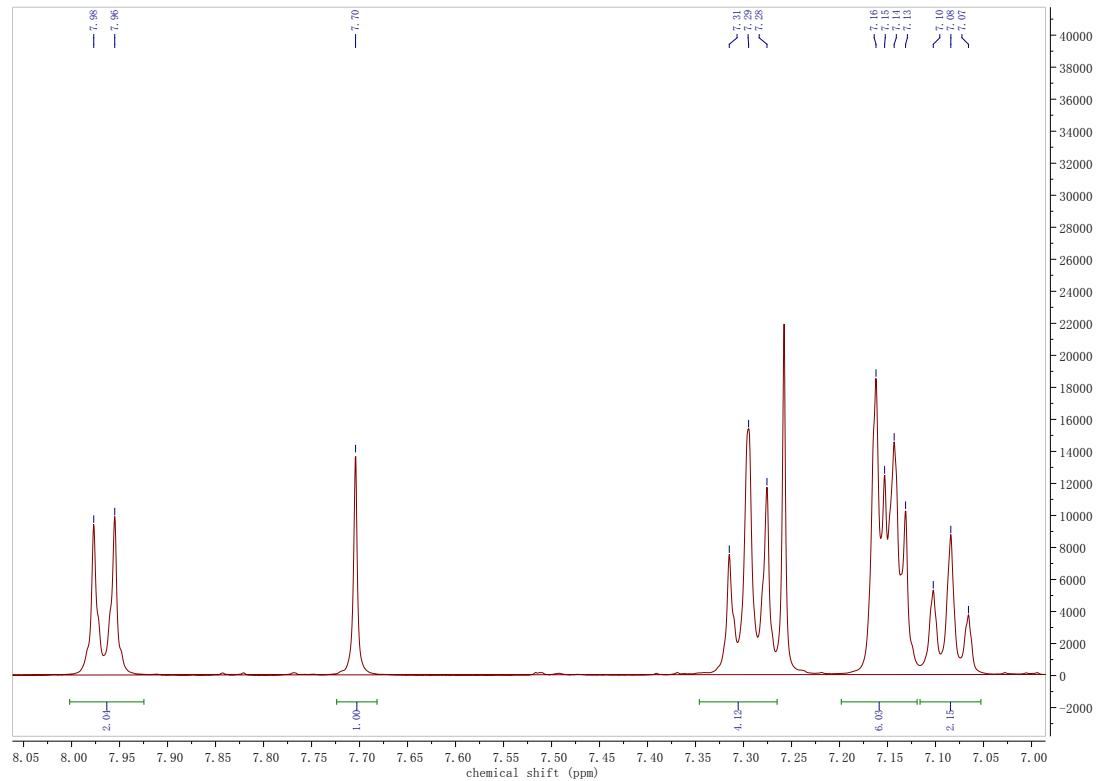


Figure S4. ¹H NMR spectrum of TPA-Py-CN.

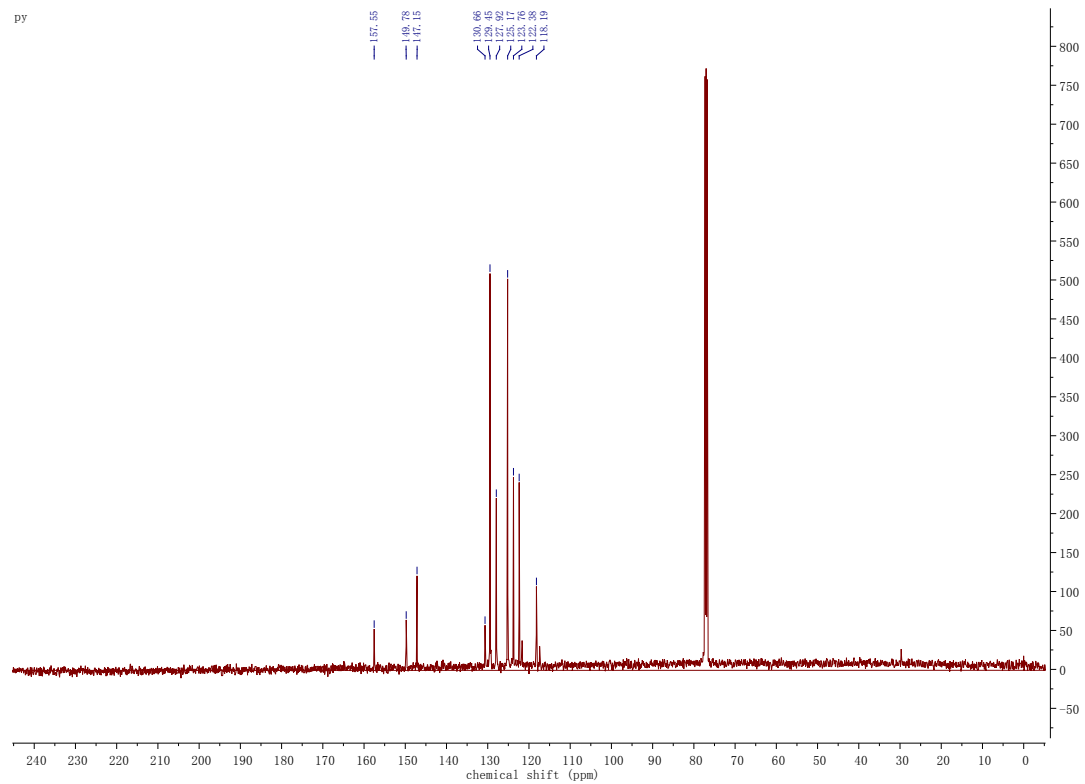


Figure S5. ^{13}C NMR spectrum of TPA-Py-CN.

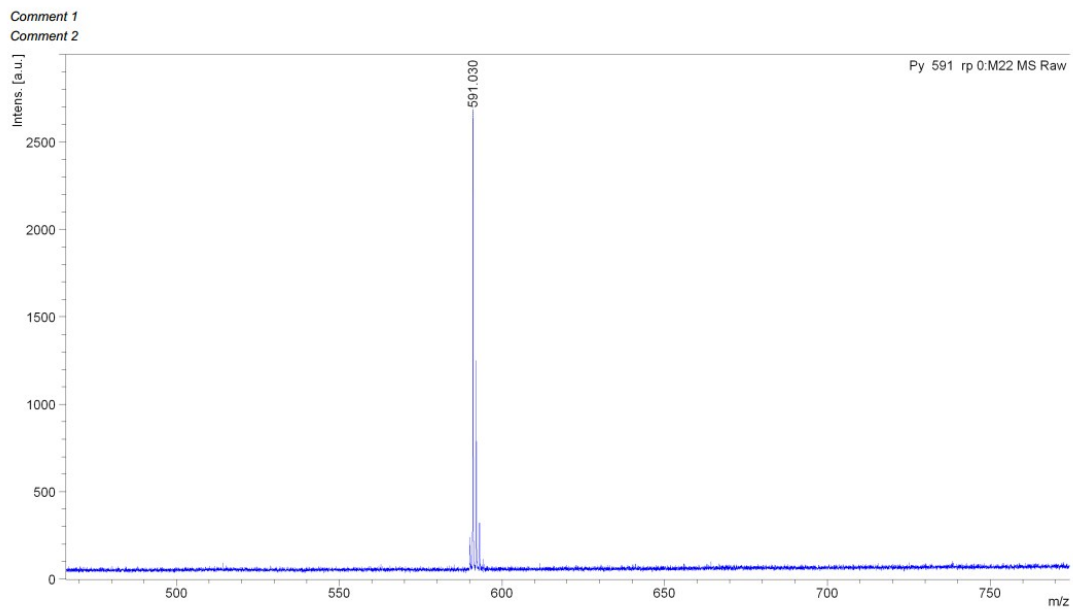


Figure S6. MS spectrum of TPA-Py-CN.

3. Single crystal parameters.

Table S1. Data summary for the obtained TPA-Ph-CN and TPA-Py-CN single crystals.

	TPA-Ph-CN	TPA-Py-CN
Sum formula	C86 H62 N6	C42 H30 N4
Formula wt	1179.41	590.70
T,K	279 K	273 K
Space group	P -1	P 1 21/c 1
Hall group	-P 1	-P 2ybc
A, Å	12.995(5)	17.2834(5)
B, Å	14.047(5)	10.2606(3)
C, Å	18.771(8)	18.3175(5)
α, deg	85.928(15)	90
β, deg	72.336(15)	96.618(1)
γ, deg	78.362(14)	90
Volume, Å ³	3198(2)	3226.74(16)
Z	2	4
Density, Mg / m ³	1.225	1.216
μ(M ₀ K α) , mm ⁻¹	0.072	0.072
R(reflections)	0.0519 (8367)	0.0631 (3776)
wR2(reflections)	0.1434 (14712)	0.2051 (7303)
Goodness of fit	0.988	0.987
CCDC	1935616	1935617

4. Raman spectra of TPA-Ph-CN and TPA-Py-CN.

Geometries and Raman simulations of TPA-Ph-CN and TPA-Py-CN molecules were based on density functional theory (DFT) and optimized *via* Becke's LYP (B3LYP) exchange-correlation functional with 6-31G (d, p) basis set.^{1,2} All DFT calculations were performed with the Gaussian 09 package.

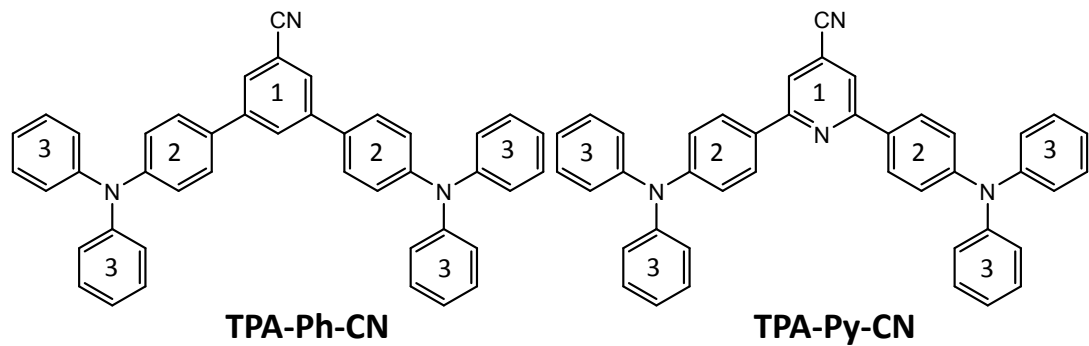


Table S2. The assignments of Raman modes of TPA-Ph-CN and TPA-Py-CN.

TPA-Ph-CN				TPA-Py-CN			
Experiment	Theory	Assignment	Experiment	Theory	Assignment		
993	1011	Triangular ring breathing vibration of Ph-1	983			Triangular ring breathing vibration of Py-1	
1001	1015	Triangular ring breathing vibration of Ph-3	1000			Triangular ring breathing vibration of Ph-3	
1012	1029	C-H rocking vibration in plane of Ph-1 and Ph-2	1008			C-H rocking vibration in plane of Py-1 and Ph-2	
-	-	-	1128		1157	C-H rocking vibration in plane of Ph-2	
1164	1196	C-H rocking vibration in plane of Ph-1	1165		1195	C-H rocking vibration in plane	
1169	1209	C-H rocking vibration in plane	1182		1210	C-H rocking vibration in plane	
1181	1223	C-H rocking vibration in plane	1192		1219	C-H rocking vibration in plane of Ph-2 and Ph-3	
-			1346		1359	C=C stretching vibration and C-H rocking vibration in plane of Ph-2 and Ph-3	
1336	1368	C-H rocking vibration in plane of Ph-3	1358		1377	C-C stretching vibration, Triangular ring breathing vibration of Py-1	
-			1541		1683	Triangular ring breathing vibration of Py-1 (C=C=N(C) stretching vibration)	

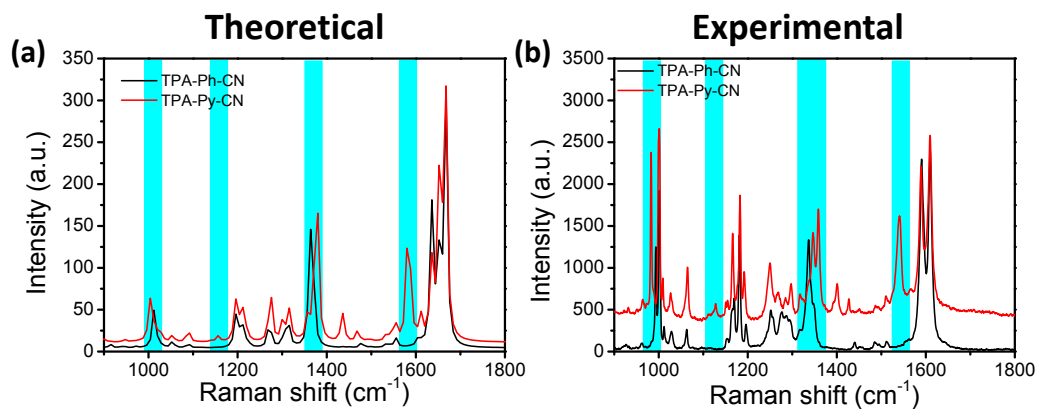


Figure S7. Comparison of Raman spectra between TPA-Ph-CN and TPA-Py-CN by theoretical simulation (a) and experimental data (b). The areas marked by blue frame in graph represent several main different Raman peaks between TPA-Ph-CN and TPA-Py-CN.

5. Absorption spectra of TPA-Ph-CN and TPA-Py-CN.

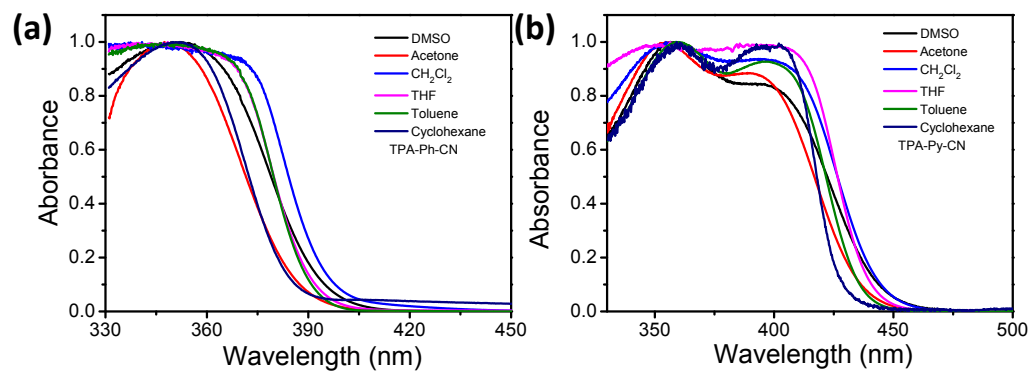


Figure S8. UV-Vis absorption of TPA-Ph-CN (a) and TPA-Py-CN (b) from nonpolar solvents to polar solvents. The concentration is 10 $\mu\text{mol/L}$ in THF.

6. HOMOs and LUMOs of TPA-Ph-CN and TPA-Py-CN.

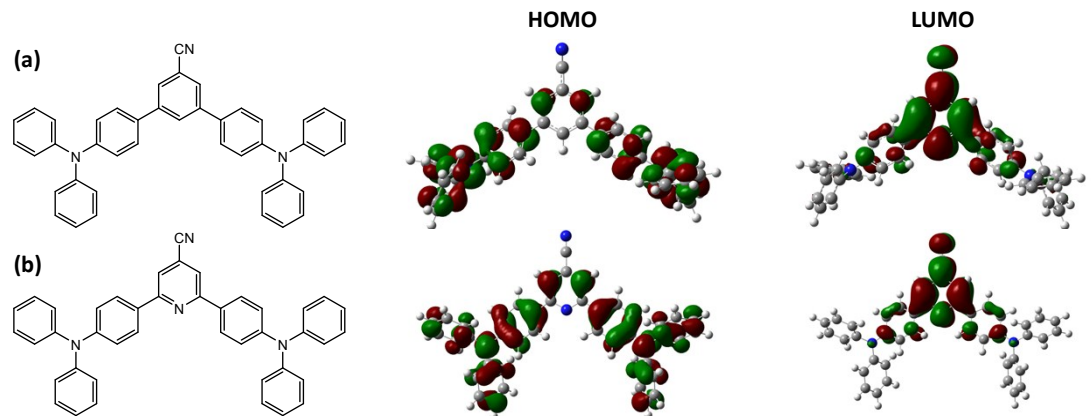


Figure S9. Optimized geometries and calculated spatial electron distributions of the HOMO and LUMO of TPA-Ph-CN (a) and TPA-Py-CN (b).

7. Fluorescent spectra of TPA-Ph-CN and TPA-Py-CN.

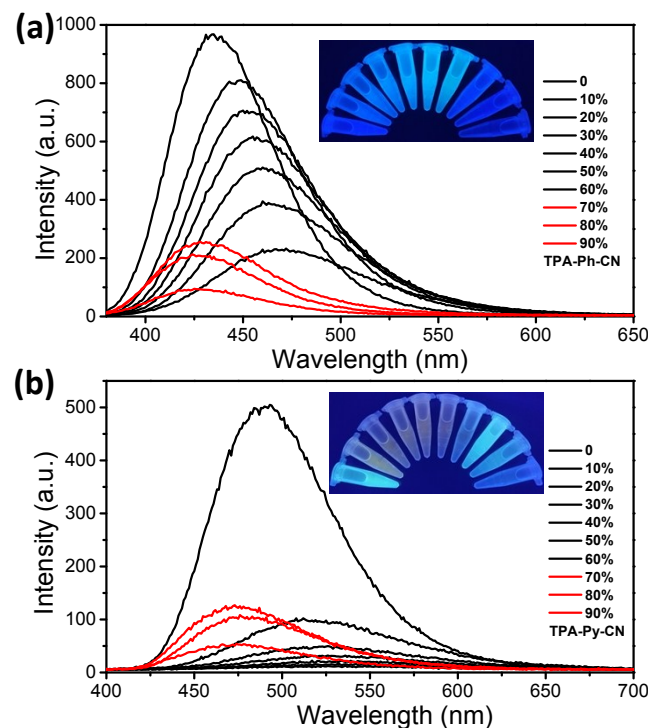


Figure S10. Fluorescence photograph and fluorescence emission spectra of TPA-Ph-CN (a) and TPA-Py-CN (b) in THF/H₂O solvents with different water fw values. The concentration is 10 $\mu\text{mol/L}$ and the excitation wavelength is 365 nm.

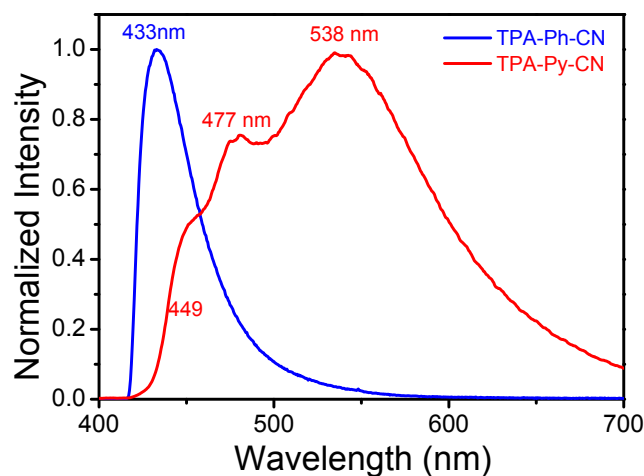


Figure S11. Fluorescent spectra in crystal forms of TPA-Ph-CN and TPA-Py-CN.

8. Structural analysis of TPA-Ph-CN and TPA-Py-CN.

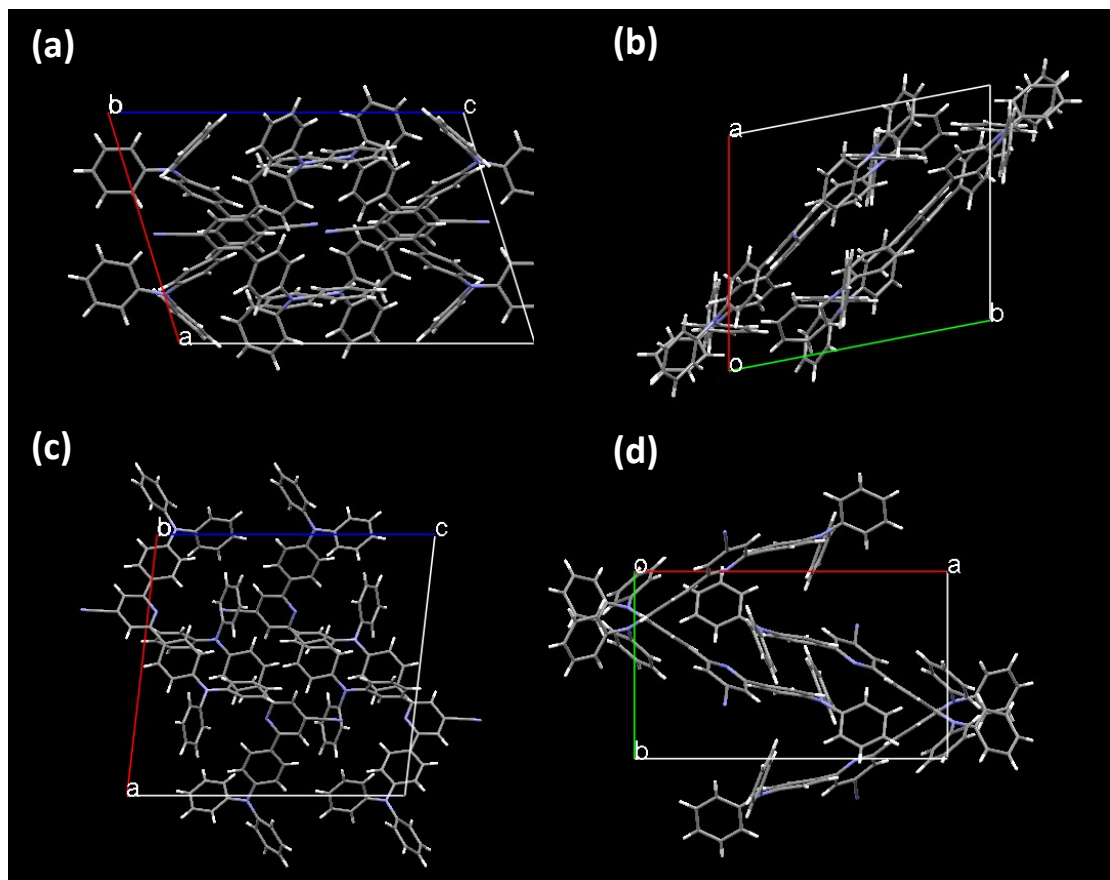


Figure S12. The unit cells in the single crystals of TPA-Ph-CN (a, b) and TPA-Py-CN (c, d).

9. Time-resolved photoluminescence (TRPL) of TPA-Py-CN.

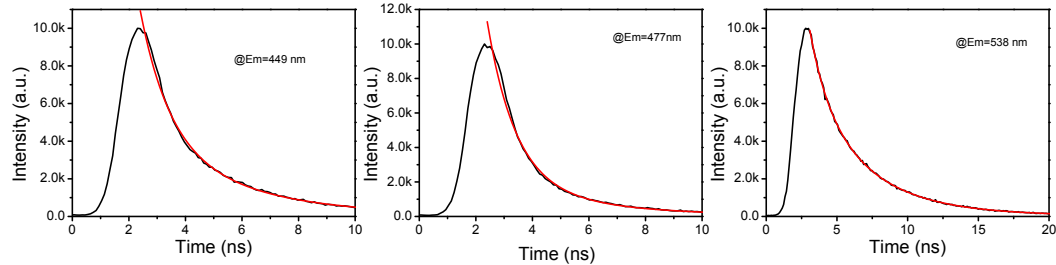


Figure S13. The time-resolved PL decay curves of TPA-Py-CN crystal. The red curves are the fitting curves by the third-order exponential decay. The excitation wavelength is 375 nm.

Table S3. Peak wavelengths and lifetimes (τ) of TPA-Py-CN crystal.

Wavelength/n m	τ_1/ns	τ_2/ns	τ_3/ns	$\tau_{\text{avg}}/\text{ns}$	χ^2
449	1.01±0.02	3.27±0.09	8.20±0.69	2.90	1.377
477	0.99±0.01	3.35±0.12	9.30±1.12	2.26	1.744
538	1.23±0.06	4.00±0.06	11.77±0.9	4.14	1.020

10. Fluorescent spectra of TPA-Ph-CN and TPA-Py-CN under hydrostatic pressure.

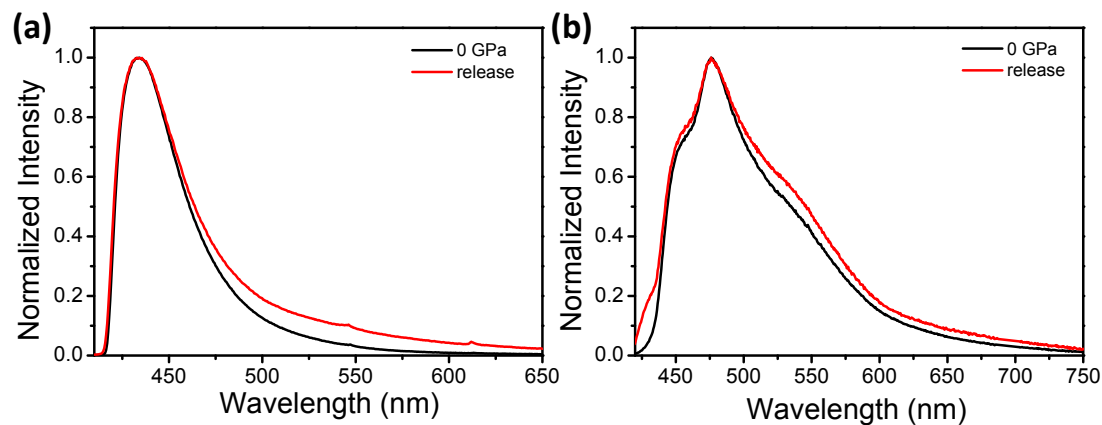


Figure S14. Comparison between the recovered and initial spectra of TPA-Ph-CN (a) and TPA-Py-CN (b). Excitation wavelength is 365 nm.

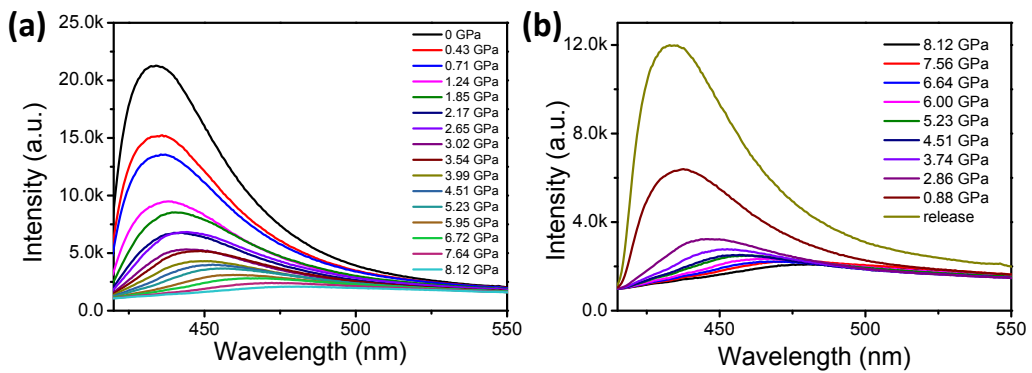


Figure S15. Fluorescent spectra of TPA-Ph-CN during compression (a) and decompression (b) *via* DAC. Excitation wavelength is 365 nm.

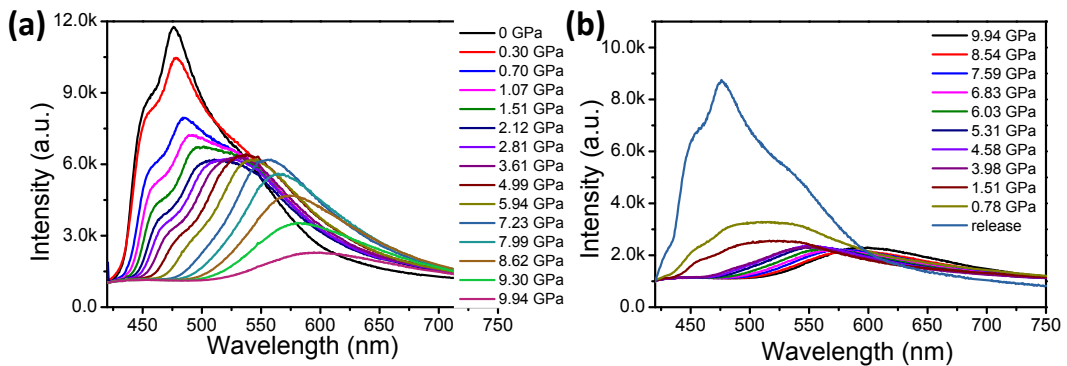


Figure S16. Fluorescent spectra of TPA-Ph-CN during compression (a) and decompression (b) *via* DAC. Excitation wavelength is 365 nm.

11. Raman spectra of TPA-Py-CN under hydrostatic pressure.

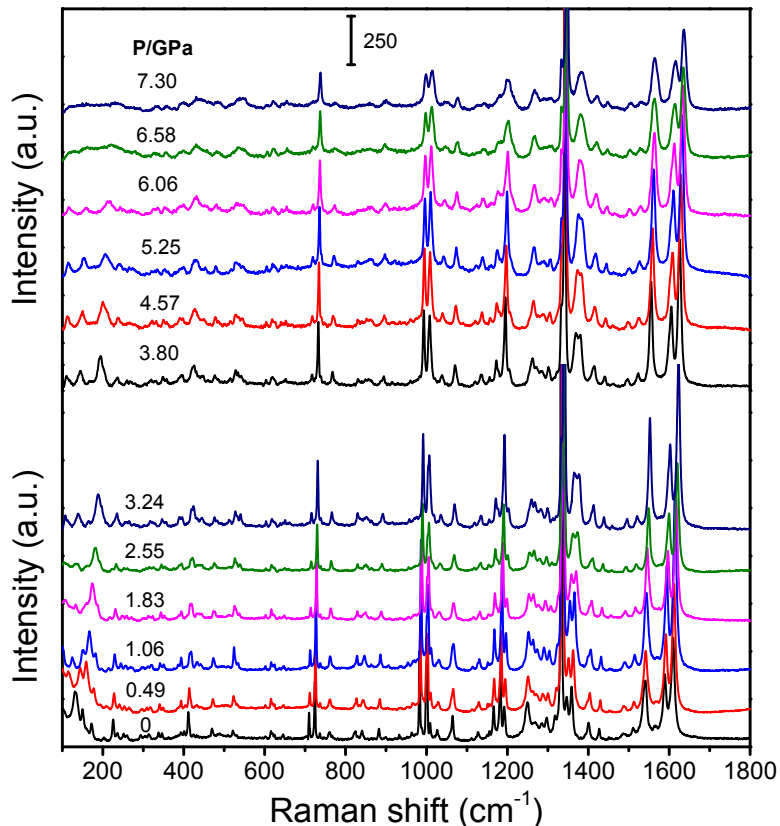


Figure S17. The high-pressure Raman spectra of TPA-Py-CN during compression. The excitation wavelength is 785 nm.

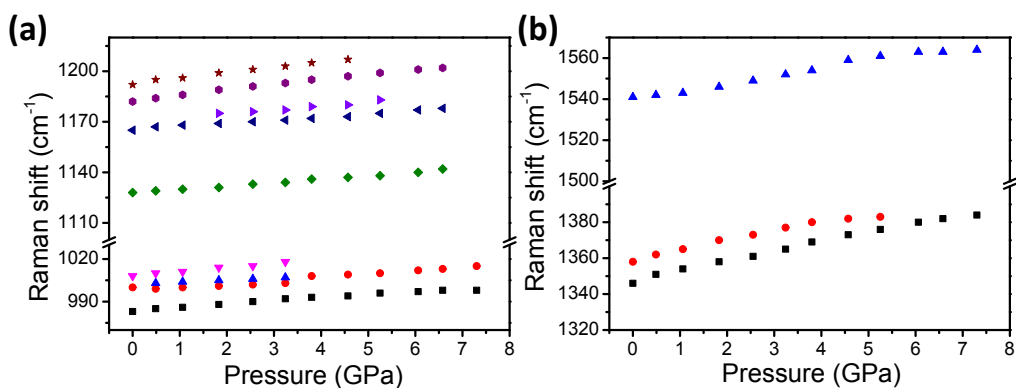


Figure S18. Raman shifts of TPA-Py-CN as a function of pressure in the ranges of (a) 970-1220 cm^{-1} and (b) 1320-1570 cm^{-1} .

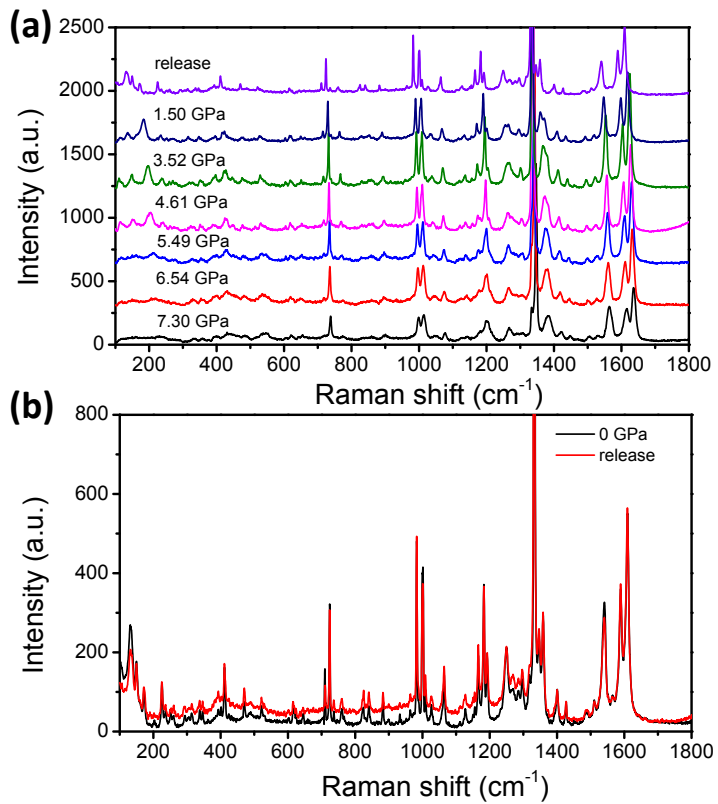


Figure S19. The high-pressure Raman spectra of TPA-Py-CN during decompression (a). (b) The comparison between initial spectrum and recovered spectrum. The excitation wavelength is 785 nm.

12. Theoretical calculations of TPA-Py-CN under pressure.

Theoretical calculation of structures with pressures was carried out by using the CASTEP package in Material Studio 7.^{3,4} This calculation was performed with a plane wave set using Norm-conserving pseudopotentials⁵ with 750 eV energy cutting off. In order to achieve geometry optimization, the energy tolerance was set as 2.0×10^{-5} eV per atom with a force tolerance of 0.05 eV/Å, a maximum displacement of 2.0×10^{-3} Å, and a maximum stress tolerance of 0.10 GPa. The energy tolerance was set as 1.0×10^{-6} eV per atom for the self-consistent field (SCF) calculation. The initial stacking modes and geometries based on the structure data of single-crystal diffraction was fully relaxed under external stress values of 0, 1.0, 2.0, 3.0, 4.0, 5.0, 6.0, 7.0 and 8.0 GPa. The generalized gradient approximation (GGA) with Perdew Burke Ernzerhof (PBE)⁶ was used to describe the exchange-correlation (XC) effects. TS scheme was used for dispersion corrections. And hirshfeld surfaces (HSs) were generated using Crystal Explorer 3.1^{7,8} based on results of the crystal data of the optimized cell units obtained from Material Studio 7.

Table S4. Optimized lattice parameters of TPA-Ph-CN under different external stress.

Stress/GPa	a/Å	b/Å	c/Å	$\alpha/^\circ$	$\beta/^\circ$	$\gamma/^\circ$	V/Å ³
Exp. Data	12.995	14.047	18.771	85.928	72.336	78.362	3198
0	14.492	15.103	19.792	87.438	72.087	86.297	4112
1	12.897	14.151	18.884	85.808	72.481	77.196	3205
2	12.505	13.863	18.652	85.625	71.845	74.235	2957
3	12.320	13.609	18.422	85.626	70.938	72.813	2788
4	12.227	13.373	18.218	85.405	70.625	71.458	2663
5	12.083	13.275	18.170	85.286	70.463	70.263	2584
6	11.947	13.208	18.078	85.159	70.181	69.262	2508
7	11.855	13.134	17.981	85.052	69.769	68.414	2440
8	11.770	13.068	17.947	84.998	69.661	67.694	2391

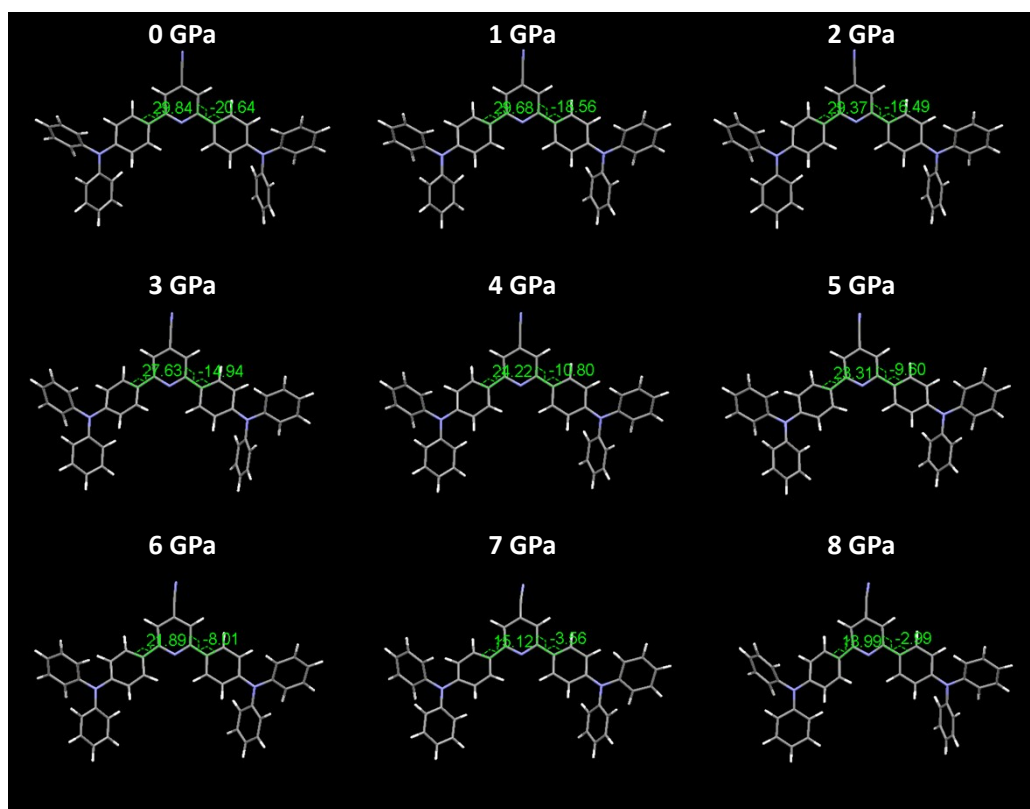


Figure S20. The detailed measurement of twisted angle of TPA-Py-CN molecule under different pressures.

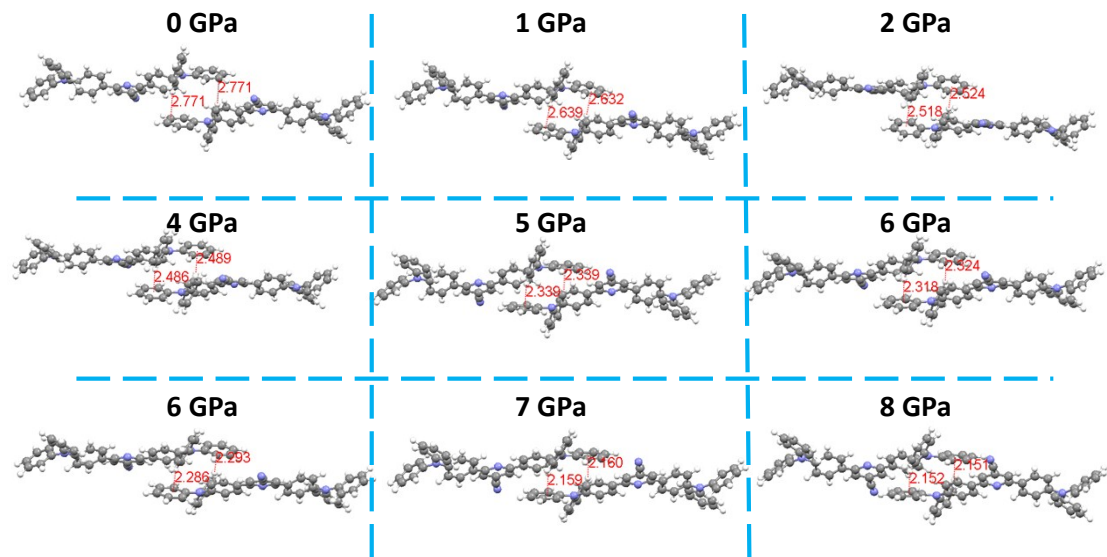


Figure S21. Calculated stacking structures of a TPA-Py-CN dimer under different pressures and the detailed measurement of distances for comparison.

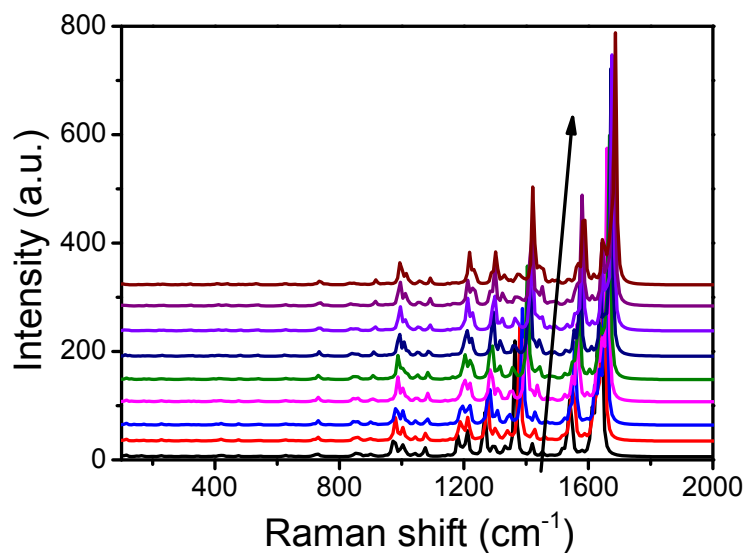


Figure S22. The calculated Raman spectra based on the structural results by Material Studio 7 under different pressures.

References

1. P. Hohenberg and W. Kohn, *Phys. Rev.*, 1964, **136**, B864-B871.
2. W. Kohn and L. J. Sham, *Phys. Rev.*, 1965, **140**, A1133-A1138.
3. B. Delley, *J. Chem. Phys.*, 2000, **113**, 7756-7764.
4. B. Delley, *J. Chem. Phys.*, 1991, **94**, 7245-7250.
5. J. P. Perdew, K. Burke and M. Ernzerhof, *Phys. Rev. Lett.*, 1996, **77**, 3865-3868.
6. G. B. Bachelet, D. R. Hamann and M. Schluter, *Phys. Rev. B*, 1982, **26**, 4199-4228.
7. L. Sun, Y. Zhao, Y. Shang, C. Sun, M. Zhou, *Chem. Phys. Lett.*, 2017, **689**, 56-61.
8. J. J. McKinnon, D. Jayatilaka and M. A. Spackman, *Chem. Commun.*, 2007, **37**, 3814-3816